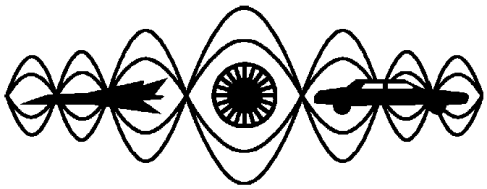

Tenth International Congress
on Sound and Vibration
7-10 July 2003 • Stockholm, Sweden

TENTH INTERNATIONAL CONGRESS ON SOUND AND VIBRATION, ICSV10

REAL TIME CONTROL OF SOUND PRESSURE AND ENERGY DENSITY IN A MINING VEHICLE CABIN

Colin H. Hansen, Daniel A. Stanef and Richard C. Morgans
Department of Mechanical Engineering, University of Adelaide, SA 5005, Australia
chansen@mecheng.adelaide.edu.au

Abstract

Real-time active noise control testing was undertaken in a cabin of a mining vehicle for the purpose of determining the relative effectiveness of energy density control vs sound pressure control. Both tonal and broadband noise over the frequency range 5 to 300Hz were used in the tests. Measurements before and after control were taken close to the error sensors and well away from the error sensors. As expected, higher reductions were achieved close to the error sensors, even when multiple sensors were used. When broadband noise was controlled, the levels at frequencies in the vicinity of the cavity resonances were reduced at the expense of increased levels at other frequencies so that the response spectrum became more flat. Energy density sensing resulted in greater levels of control than pressure sensing at distances further than approximately 300 mm from the error sensors.

1. INTRODUCTION

Drivers subjected to extended periods of exposure to low frequency noise in the cabins of heavy machinery such as diesel-driven mining vehicles experience fatigue and high levels of distraction. One possible approach to ameliorating the problem is to use active noise control (ANC). Here, the effectiveness of applying an ANC system to a Caterpillar

mining vehicle cabin is investigated using the Causal Systems EZANC II real time controller. Both energy density sensors and pressure sensors are used to provide error signals to the controller and both tonal and broadband noise spectra are used as the primary noise disturbance. Random noise excitation was first generated by the EZ-ANC II and subsequently a recording of existing cabin noise was used with the intention of simulating as closely as possible the actual noise environment in a typical mining vehicle.

In a previous paper[1], a finite element analysis undertaken on the experimental cabin was used together with measurements of the transfer functions between control sources and error sensors to predict the feasibility of a number of alternative sensing strategies for achieving both global and localised noise reductions in the cabin. Results from the analytical work indicated that ANC could produce zones of local control inside the cabin for both energy density and sound pressure sensing strategies, with a larger "zone of quiet" about the error sensors predicted with the energy density sensing strategy. The work also showed that for a single local primary acoustic source in the cabin, it was not possible to achieve global control using other acoustic sources and error sensors distributed around the cabin, even if the number of control sources and error sensors was very large. Experimental work reported here demonstrates the relative effectiveness of sound pressure sensing vs energy density sensing for achieving noise reductions in the local region near the driver's head.

2. EXPERIMENTAL ARRANGEMENT AND PROCEDURE

The experimental arrangement is shown in Figure 1. The system used the Causal Systems EZANC II controller as a basis. For each test that used the sound pressure sensing technique, signals from four low-cost electret condenser microphones located in the cabin and amplified via custom built amplifiers were directed to the controller. The locations of the four error sensor microphones, which were positioned close to the driver's head location, are labelled "EH" and are shown in Figure 2. Also shown in Figure 2 are the locations of the energy density probe (near the driver's head location and labelled "ED") and the location of the monitor microphone ("MED") used for monitoring the sound pressure level at the location of the energy density probe. The sound pressure reduction at this monitor microphone, measured during ANC experiments with the energy density sensor, was used as a comparison with the average sound

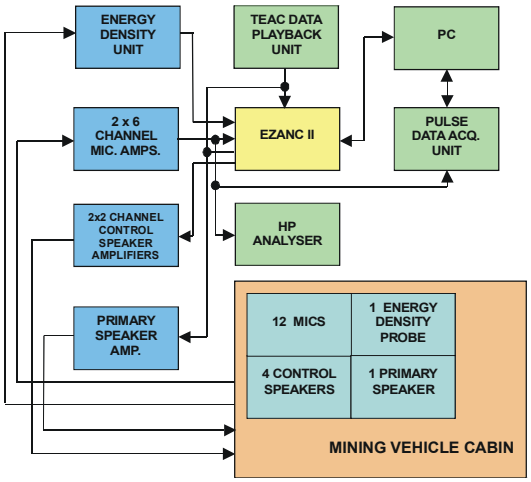

Figure 1. Flow diagram of experimental arrangement.

pressure reduction at the four error microphones achieved during ANC experiments using the sound pressure sensing strategy.

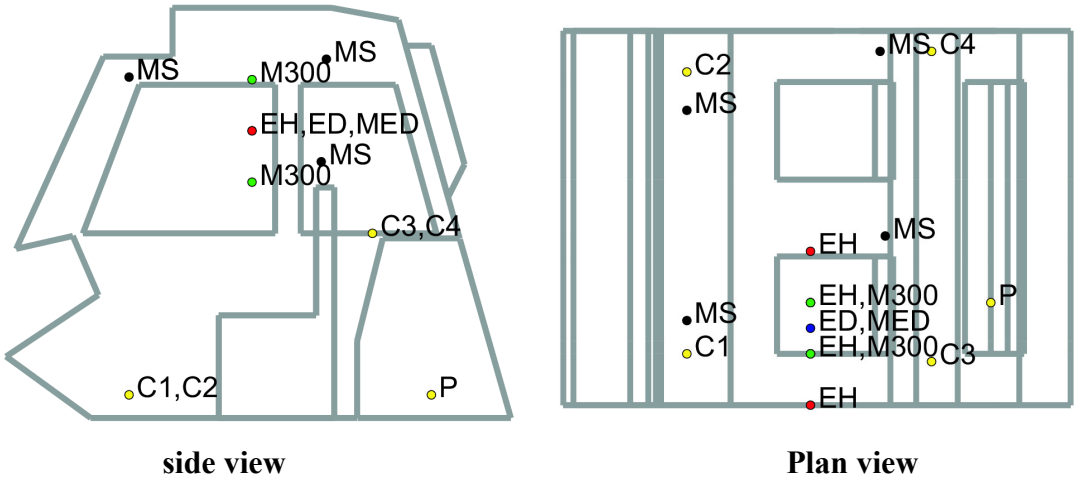

Figure 2. Locations of primary source (P), control sources (C1…C4), microphones within 300 mm of nearest error sensor (M300), randomly spaced microphones located further than 300 mm from the nearest error sensor (MS), error sensor microphones near driver's head location (EH), energy density probe (ED) and microphone at the centre of the energy density probe (MED).

For tests using the energy density sensing strategy, the signals from the four microphones of the energy density probe were pre-processed to provide three orthogonal velocity signals and one pressure signal, which were then used as input signals to the EZANC II controller, as shown in Figure 1.

The locations of the eight monitor microphones, which were used during ANC experiments with both sensing strategies to measure the extent of the zone of quiet around the error sensors during control, are shown in Figure 2. The monitor microphones that were within 300 mm of the nearest error sensor are labelled, "M300" and those that were randomly spaced throughout the cabin at distances larger than 300 mm from the nearest error sensor are labelled, "MS".

The loudspeakers that were driven by the EZ-ANC II outputs were located as shown in Figure 2 at positions labelled "C1….C4". All four control speakers were used for every test. The primary acoustic source, identified as "P" in Figure 2, was positioned in the boot of the cabin.

The first step in each test was to perform cancellation path modelling using the reference signal. For tonal noise this was completed automatically by the ANC software, but for random noise, the cancellation path identification was performed manually by using the "view weights" feature of the software and waiting for convergence to occur.

Tonal primary disturbance tests were undertaken at 53 Hz , 65 Hz and 111 Hz with and without the first and second harmonics. However, only results for the 55 Hz tests are shown here. In addition, tests were also conducted for band limited random noise (0-300 Hz) and for a noise signal actually recorded in a typical vehicle cabin on-site.

Every primary noise type was controlled first using the energy density sensing strategy, and then the sound pressure sensing strategy. For both strategies four error sensors and four control sources were used, with the error sensors located in the vicinity of the driver's head location, and the control sources in the front and back corners of the cabin as shown in Figure 2.

3. RESULTS

The primary and controlled sound fields for each test are shown in Figures 3 to 5. Each figure comprises six graphs. The left most graphs correspond to the pressure sensing strategy and the right most graphs correspond to the energy density sensing strategy. The top two graphs in each figure correspond to the sound pressure sensed by the microphone at the energy density probe or the average pressure at the four error sensors, depending on whether the results are from an energy density or sound pressure sensing strategy test. The centre two graphs represent the average response of four microphones at 300 mm from the energy density probe or nearest pressure error sensor. The bottom two graphs represent the energy average of the sound pressure levels measured by the four microphones positioned randomly in the cabin and further than 300 mm from the nearest error sensor.

4. ANALYSIS

By combining the reductions achieved for various primary disturbance frequencies, the sound pressure sensing strategy emerges as the preferred strategy for achieving higher levels of reduction at the error sensors and at distances closer that 300 mm from the error sensors. Energy density sensing out-performs sound pressure sensing in terms of the level of reduction achieved at positions far away from the error sensors (ie. "at microphones spaced throughout cabin") and also results in a smaller controlled pressure gradient in the vicinity of the error sensors. A large pressure gradient is undesirable because it results in large changes in perceived sound pressure level as the driver moves his/her head around within the "zone of quiet". Energy density sensing was found to produce a larger and more uniform zone of quiet than sound pressure sensing; this outcome agrees with the findings of the FEA analysis on mining vehicle cabin noise reported previously[1].

As was expected, greater levels of reduction are achieved when the cabin is excited at or near its resonance frequency of 53 Hz and these results are illustrated in Figure 3. The sum totals of reductions across the three groups of microphones tested were found to

be significantly higher for the 53 Hz and 65 Hz primary tone cases than the 111 Hz primary tone case. These latter results are not shown here due to lack of space.

In some instances, when only the fundamental tone was included in the reference and primary signals, application of ANC resulted in slight increases in the levels at frequencies corresponding to the first and second harmonics, due to harmonic distortion of the speaker response. For this reason the experimental work was repeated with the first and second harmonics included as part of the disturbance and reference signals. This resulted in similar levels of control of the fundamental without the observed increase in level at the second and third harmonics. These latter results are included in Figure 3.

With random primary noise generated by the controller, sound pressure sensing achieved greater reduction over certain frequency bands within the spectrum (40 – 80 Hz, 120 – 140 Hz, and 230 – 280 Hz). However, this was offset by the increase in noise level at other frequencies. Results are shown for both sensing strategies in Figure 4.

When excited with the tape recording of on-site cabin noise, both sensing strategies achieved a significant reduction of the peak at 53 Hz and surrounding frequencies, but also increased the noise level over the 100 Hz to 250 Hz range. These results are shown in Figure 5.

It is clear from all three figures that the amount of achievable noise reduction steadily reduces as the measurement location becomes further from the error microphones. This was predicted by the analytical work reported previously[1].

5. CONCLUSIONS

By using a four-sensor, four-control source real time ANC system, attenuation of tonal and broadband primary disturbances was achieved inside a mining vehicle cabin using energy density and sound pressure sensing strategies. Reduction of tonal disturbances was achieved using both strategies, with sound pressure sensing outperforming its counterpart at locations up to 300 mm away from the error sensors. When the energy density sensing strategy was used, higher levels of attenuation were achieved at locations in the cabin further away from the error sensors.

When broadband control was implemented, reductions at frequencies at and near the low-frequency resonances of the acoustic cavity were achieved at the expense of increasing the noise level at other frequencies. This occurred for both sensing strategies. The use of more error sensors and control sources has the potential to lead to a greater level and larger zone of control in the cabin, as could alternative positioning of the control system sensors and actuators.

REFERENCE

Hansen, C.H., Stanef, D.A. and Morgans, R.C. (2002). Active control of low frequency sound in a mining vehicle cabin. Proc. 2002 Annual Conference of the Australian Acoustical Society, Adelaide, South Australia, Nov. 13-15.

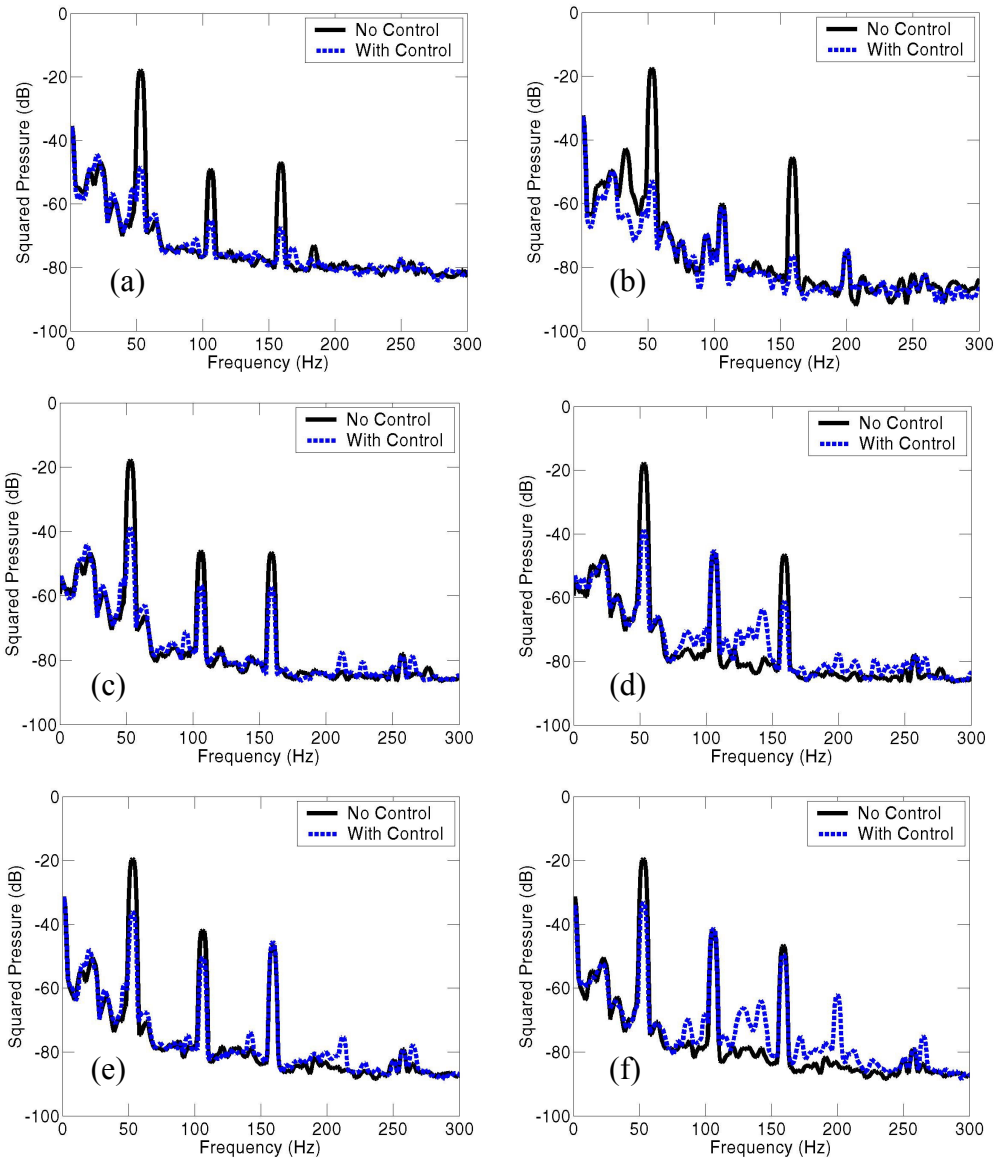

Figure 3. Real time ANC results for the mining vehicle cabin, showing sound pressure levels before and after control. Excitation consists of a 53 Hz tone and the first two harmonics. Figures (a), (c), and (e) show the results the sound pressure sensing strategy and Figures (b), (d) and (f) show the results for the energy density sensing strategy. Figure (a) shows the average of the sound pressure sensed by the 4 error microphones; Figure (b) shows the sound pressure sensed by the microphone located adjacent to the ED probe; Figures (c) and (d) show the sound pressure level averaged over the four monitor microphones within 300 mm of the furthest error sensor; and Figures (e) and (f) show the sound pressure level averaged over the four monitor microphones distributed throughout the cabin at a distance of at least 300 mm from the nearest error sensor.

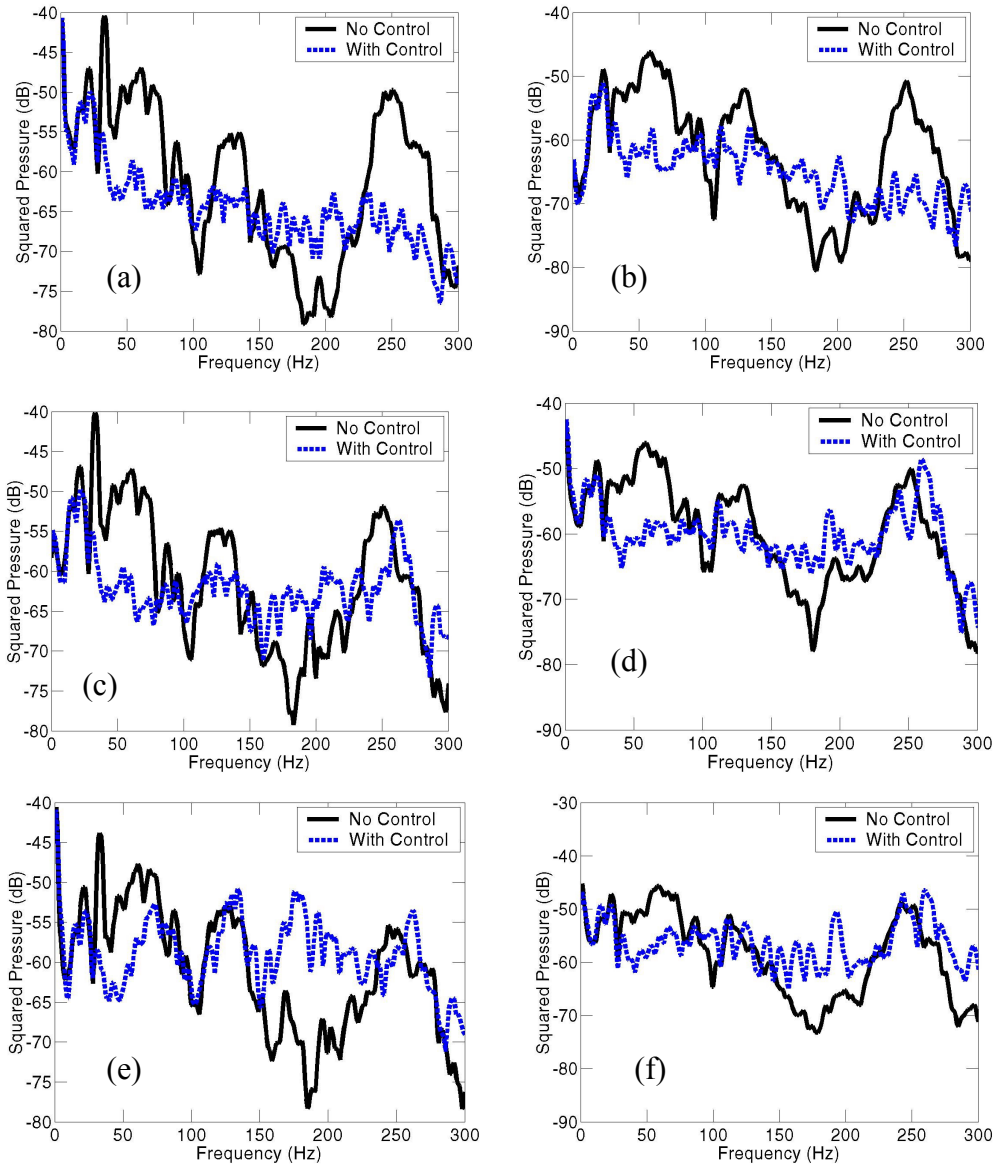

Figure 4. Real time ANC results for the mining vehicle cabin, showing sound pressure levels before and after control. Excitation consists of band limited random noise between 0 and 300 Hz. Figures (a), (c), and (e) show the results the sound pressure sensing strategy and Figures (b), (d) and (f) show the results for the energy density sensing strategy. Figure (a) shows the average of the sound pressure sensed by the 4 error microphones; Figure (b) shows the sound pressure sensed by the microphone located adjacent to the ED probe; Figures (c) and (d) show the sound pressure level averaged over the four monitor microphones within 300 mm of the furthest error sensor; and Figures (e) and (f) show the sound pressure level averaged over the four monitor microphones distributed throughout the cabin at a distance of at least 300 mm from the nearest error sensor.

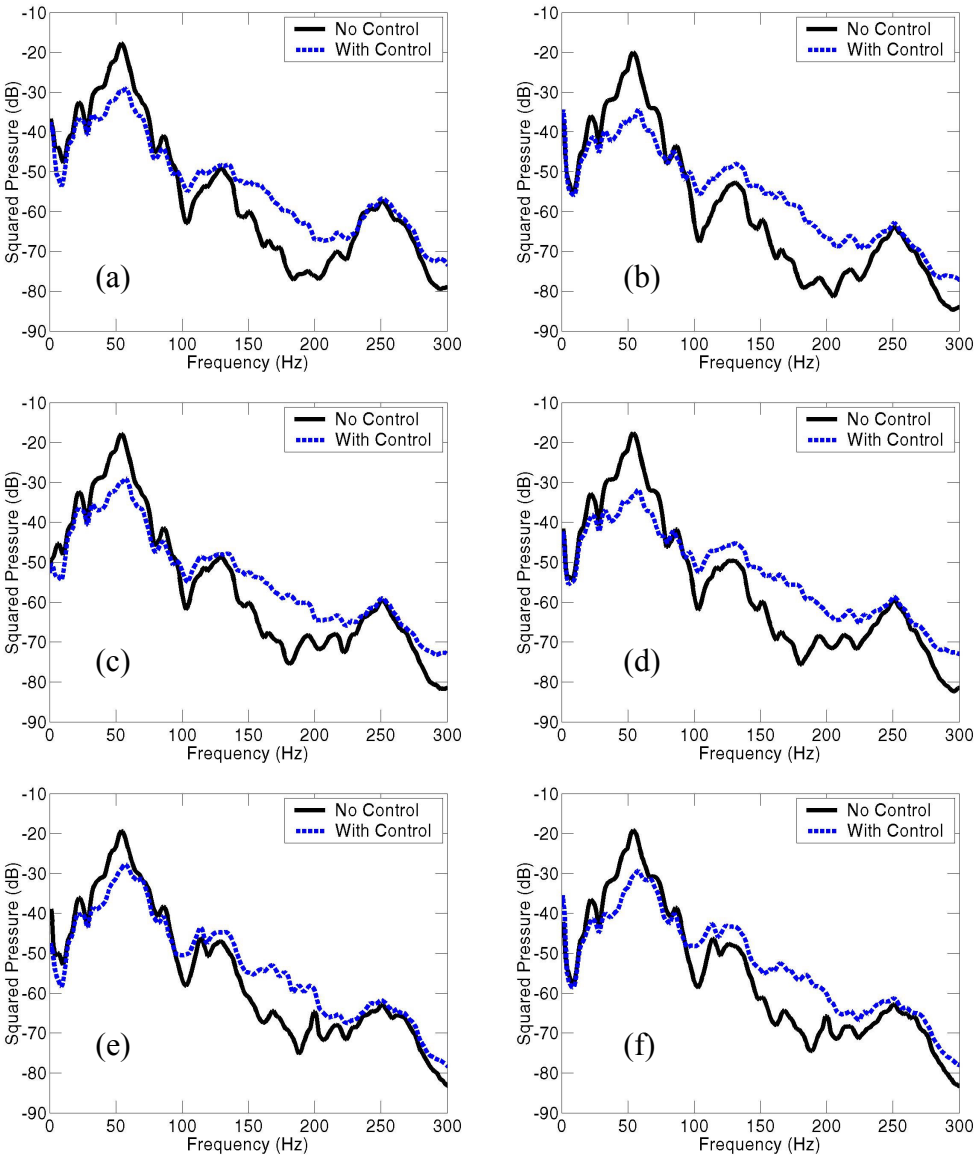

Figure 5. Real time ANC results for the mining vehicle cabin, showing sound pressure levels before and after control. Excitation consists of noise recorded in a mining vehicle cabin and band limited to 300 Hz. Figures (a), (c), and (e) show the results the sound pressure sensing strategy and Figures (b), (d) and (f) show the results for the energy density sensing strategy. Figure (a) shows the average of the sound pressure sensed by the 4 error microphones; Figure (b) shows the sound pressure sensed by the microphone located adjacent to the ED probe; Figures (c) and (d) show the sound pressure level averaged over the four monitor microphones within 300 mm of the furthest error sensor; and Figures (e) and (f) show the sound pressure level averaged over the four monitor microphones distributed throughout the cabin at a distance of at least 300 mm from the nearest error sensor.